

Ray Tracing Investigation of Plasma Gratings

Emily Warne¹ and David Neely²

¹Central Laser Facility, now University of Southampton

²Central Laser Facility

Based on the success of plasma mirrors as optics in high intensity laser systems, the possibility of forming a diffraction grating from a plasma in a similar manner was investigated. A ray tracing simulation was written in MATLAB for this purpose, and was used to find the path of light rays interacting with a plasma mirror and various models of plasma grating.

Plasma mirrors are well established as optics in high intensity laser systems. They are effective reflectors at intensities that would destroy other, conventional optics, and additionally can provide many beneficial effects on the properties of a pulse [1].

Under the right conditions, the reflectivity of a plasma mirror can be very high. For a single pulse, which creates the plasma mirror and is then reflected by it, reflectivities of up to 80% have been observed [1]. This reflectivity was seen for a plasma mirror produced from a fused silica surface by a 90 fs, 800 nm pulse incident at an angle of 6°. The reflectivity was shown to be dependent on incident angle, pulse length, and intensity. The threshold intensity for plasma mirror formation was 10^{14} W/cm² for a 90 fs pulse, with the optimum reflectivity in the range of 3×10^{15} – 3×10^{16} W/cm².

The reflectivity of a plasma mirror can be further enhanced by using a prepulse to form it and allowing the plasma to expand for a short time before reflecting the main pulse from it [2]. A reflectivity of 96% has been achieved for 1054 nm, 500 fs pulses, with a prepulse:main-pulse ratio of 1:8. The optimum time delay between pulses was shown to be 3 ps, corresponding to a plasma density scale length of 0.3 μ m at the time of the main pulse. The reflected beam was also observed in the far field, and time delays up to 3 ps were seen to produce a comparable spot size to that from a single pulse. Longer time delays produced increased spot sizes, with an order-of-magnitude decrease in equivalent intensity for a 10 ps time delay.

The principle of plasma mirrors has also been used to produce transient plasma gratings, by interfering two 800 nm, 25 fs prepulse beams with a peak fluence of 1.7×10^2 J/cm² onto a silica target. The plasma structure was then probed by producing harmonics on the grating via high harmonic generation and observing the resulting diffraction pattern in the harmonics. It was seen that the periodicity of the grating could be

controlled by the focusing configuration, and the grating depth controlled by the time delay between pulses. A typical grating period was 7 μ m, and the maximum achievable grating depth before smearing of the structure by hydrodynamical expansion was on the order of the laser wavelength [3].

This report discusses ray tracing simulations of various proposed forms of plasma grating, with the aim of finding a periodic plasma structure that will act as an effective and efficient grating. A potential use for this is in pulse compression, which requires a high line density. The simulation code was initially tested on a simple plasma mirror model, as the results could be compared to known behaviour and to a ray path equation derived from Snell's Law. Then simulations were run to investigate the behaviour of a sinusoidal grating, a triangular grating produced by a Fourier series sum, and a hypothetical rounded sawtooth grating.

The MATLAB ray tracing code takes an equation for the two-dimensional electron density being tested, and moves the position of the ray forwards in a number of small steps (maximum step length = 10 nm), changing its path according to Snell's Law after each step. The code does not account for the expanding motion of the plasma, as this is effectively negligible given the speed of light and the micrometre scales involved.

Plasma Mirror

The electron density distribution is treated as constant parallel to the ionised surface (a reasonable approximation on small scales) and as exponentially decreasing with distance from the surface. For a plasma with scale length L , formed from a surface along $y = 0$, the electron density is given by:

$$n_e = n_{e0} e^{-y/L} \quad (1)$$

The refractive index of the plasma varies as a function of electron density:

$$n_{ref} = \sqrt{1 - \frac{n_e q_e^2}{\epsilon_0 m_e \omega^2}} \quad (2)$$

where q_e is the electronic charge, ϵ_0 is the permittivity of free space, and ω is the angular frequency of the light. The refractive index decreases with proximity to the surface of the plasma. A distance is reached where

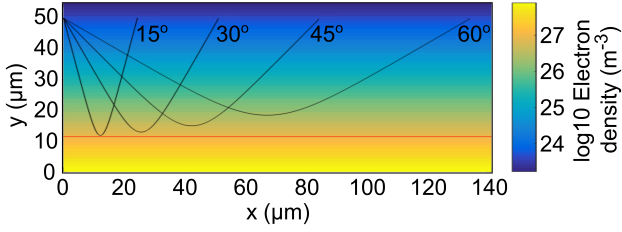


Figure 1: Paths of rays incident at a variety of angles onto a plasma mirror.

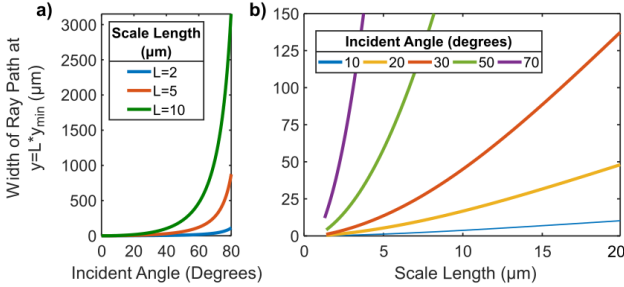


Figure 2: Graphs showing the effects of [a] incident angle and [b] scale length on the width of the ray path, measured at a y value defined by the scale length L , and the y coordinate of the ray's turning point, y_{\min} . It can be seen that the ray path is much wider at larger incident angles and that there is a fairly steady increase in ray path width with scale length, at all angles.

$\frac{n_e q_e^2}{\epsilon_0 m_e \omega^2} = 1$, and the refractive index is therefore zero. This is the critical surface, beyond which light of a particular frequency cannot propagate. In our model of a plasma mirror, it is described simply by a value of y .

It can be seen from Figure 1 that, as with a standard mirror, the angle of incidence is equal to the angle of reflection for a plasma mirror. Unlike a standard mirror, the ray path is curved as it travels through the plasma with its smoothly changing refractive index. The shape of the ray path and the proximity of the minimum point of the ray to the critical surface are dependent on the incident angle and the scale length of the plasma. A ray path width can be defined by considering a line with a constant, selected value of y and finding the distance between the two points where the ray path crosses this line. The effects of incident angle and scale length on this ray path width are shown in Figure 2.

Further to the ray tracing simulation, an equation can be found for the ray path [4]. This allows the effects of various parameters, like scale length and incident angle, to be more easily and precisely determined.

$$y = -L \ln \left[\frac{n_e}{n_c} (1 - k^2) \operatorname{sech}^2 \left(\frac{\sqrt{1 - k^2}}{2Lk} (x - C) \right) \right] \quad (3)$$

where $C = x_0 - \frac{2Lk}{\sqrt{1 - k^2}} \operatorname{arctanh} \left(\sqrt{1 - \frac{n_{e0}}{n_c} \frac{e^{-y/L}}{(1 - k^2)}} \right)$

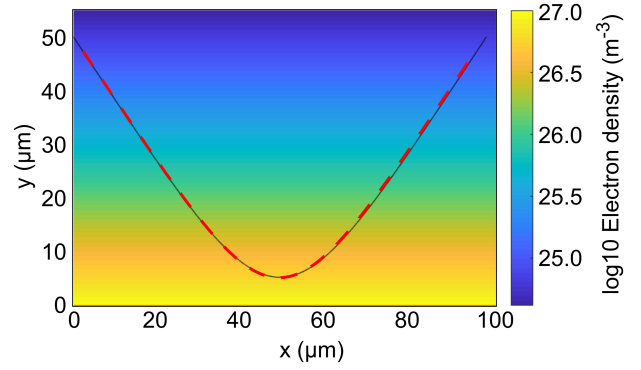


Figure 3: The ray path from Equation 3 (red dashed line) and the ray path calculated by the simulation (black line) for the same parameters.

where n_c is the critical density and $k = n_0 \sin(\theta_0)$, with n_0 being the refractive index of the plasma at the start of the ray, and θ_0 being the initial angle of the ray to the electron density normal. Figure 3 shows the ray path calculated from this equation plotted on top of the result of the simulation, and it can be seen that they match very well.

The derivation of this equation can be found in Appendix A.

Plasma Gratings

There are two main properties of a grating we are concerned with here:

1. that it has some periodic structure,
2. that the angle of the reflected rays is consistent, and different to the incident angle.

Sinusoidal Grating

A sinusoidal electron density could be created by interfering beams onto the surface to be ionised. Such a plasma would have a periodic structure, meeting the first of the grating conditions. The electron density of this plasma structure was modelled to be tested for the second of the grating properties. The equation used was:

$$n_e = \left[n_c + n_{amp} \frac{2p}{y} \sin^2 \left(\frac{\pi x}{p} \right) \right] e^{-y/L} \quad (4)$$

with p being the period of the sinusoid. Simulations were first done without the $2p/y$ term, meaning the plasma was expanding in the y direction only. The $2p/y$ term was then added to give the model a more realistic expansion, so the plasma was expanding in the x direction as well.

It was found, however, that a sinusoidal electron density does not meet the second criterion at all well. Figure 4 shows typical ray traces for this sinusoidal grating in a number of different regimes.

At large incident angles (a), a ray samples too many grating periods for the sinusoidal structure to have an

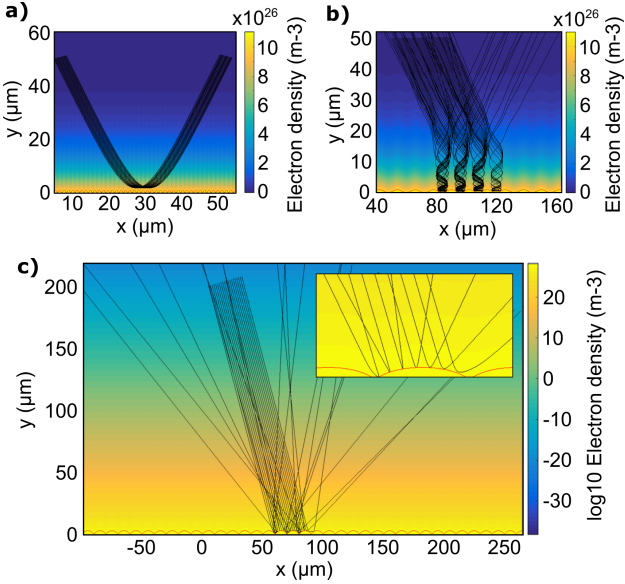


Figure 4: [a] In the large-angle case, the ray samples many grating periods and is reflected as if by a plasma mirror. [b] For very small angles, the ray is ‘captured’ by the grating. [c] In a typical moderately-small incident angle ray trace for a sinusoidal grating, the rays are reflected across a wide range of angles.

effect, and the ray is reflected much like it would be from a simple plasma mirror. The threshold angle for this regime varies by plasma scale length, and may be as low as 20° .

At very small incident angles (b), the ray gets ‘captured’ by the grating; it reflects repeatedly off the sides of one of the periods of the sinusoid, eventually escaping in a direction extremely sensitive to the exact path of the ray. This means a collimated beam ends up being spread across a large range of angles.

The more realistically expanding model is less susceptible to the ray capture problem, but even with the rays reflecting only from the peaks of the sinusoid (c), they are reflected across a very large range of angles. It would seem that this is due to the curved shape of the sinusoid.

Triangular & Sawtooth Gratings

Since the curved shape of a sinusoid causes the rays to be reflected across a large range of angles, a structure with straighter edges is likely to be more effective. An initial idea was to produce such a structure with a Fourier series sum, as this could potentially be produced experimentally by interfering a number of beams together in the right configuration. The idea of a Fourier series sum structure was tested with a triangular waveform. (See Appendix B.1 for equation.)

Triangular Waveform - Fourier Series Sum

The accuracy with which a Fourier series sum can approximate a perfect triangular wave depends on the order of the sum, i.e. the number of terms in the series. A sum of fewer terms provides a lower accuracy but

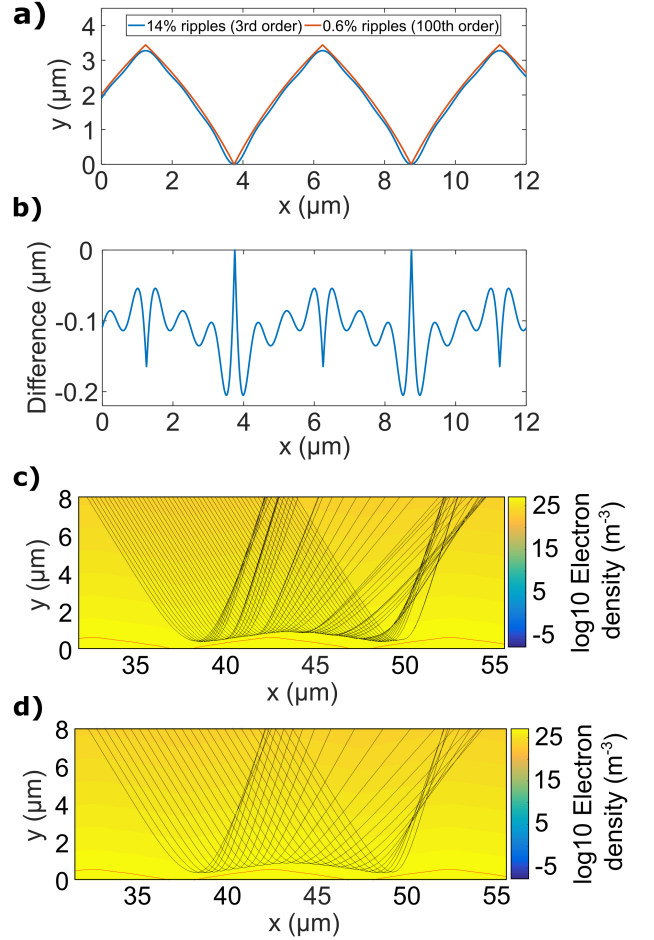


Figure 5: [a] The shape of the critical surface for low (3rd) order and high (100th) order sums. [b] The difference between the low order position of the critical surface and that of a perfect triangular wave. [c] Ray trace from a 3rd order triangular structure. While the rays are reflected in roughly the same direction, there is a lot of variation in the angle. [d] Ray trace from a 100th order triangular structure. The rays are reflected at a much more uniform angle, but there is still noticeable variation.

is also more experimentally feasible. Because of these competing factors, both a low order and a high order sum were tested, to demonstrate the most experimentally simple option and compare this to the best that could reasonably be achieved with the Fourier series idea.

Figure 5 shows the results of the Fourier series sum simulations. The shapes of the low and high order waveforms (a) are visibly different. A 3rd order Fourier sum (the sum of three sinusoids) has ripples in the critical surface (b) that deviate from a perfect triangular wave by 14% on average. If a collimated beam is incident on the structure (c), the directions of the reflected rays differ from one other to a great extent. Even for a 100th order sum (d), with ripples of 0.6% on average, there is a noticeable variation in the directions of the reflected rays. It is apparent that the path of the rays is extremely sensitive to non-uniformities in the plasma, particularly at the turning point. However, the rays are reflected in broadly the same direction,

indicating that a straight-edged structure is likely to be effective.

While it seems that a Fourier series sum is not the way forward, this (approximately) straight-edged shape has produced the best results yet. It makes sense, therefore, to find a structure that would work as a grating, and then try and work out how to produce it in a plasma.

Rounded Sawtooth

Since with the triangular waveform the rays are reflected from both sides of the peaks, the obvious shape to try next is a sawtooth wave — rather like a blazed grating. A rounded sawtooth function [5] is used, since this avoids discontinuities in the plasma, which would be non-physical. (Conveniently, it is also differentiable everywhere, unlike a standard sawtooth function.) The electron density is given by:

$$n_e = [n_c + n_{amp} \text{saw}(x)] e^{-y/L} \quad (5)$$

The function $\text{saw}(x)$ is given in Appendix B.2.

The scale length, L , is varied periodically with x , since the end of the plasma that has expanded further is hotter, and has a larger scale length. This also compensates for the curving of the top of the sawtooth caused by the expansion of the plasma, as shown in Figure 6.

$$L = L_{min} + L_{amp} \text{saw}(x) \quad (6)$$

The majority of the rays in a collimated beam incident on this plasma structure are reflected in the same direction, which is different to the angle of incidence. However, rays incident at the edges of the sawtooth are bent by the sudden change in refractive index, and are reflected across a large range of angles. This is shown in Figure 7. The proportion of rays deflected non-uniformly from the edge of the sawtooth rather than reflected from the flat surface is dependent on the grating period, as shown in Figure 8. For a sufficiently large grating period, the majority of the rays are deflected at the same angle, which is different to the incident angle. This angle is also wavelength-dependent, as shown in Figure 9. A sawtooth wave electron density therefore meets the criteria for a grating.

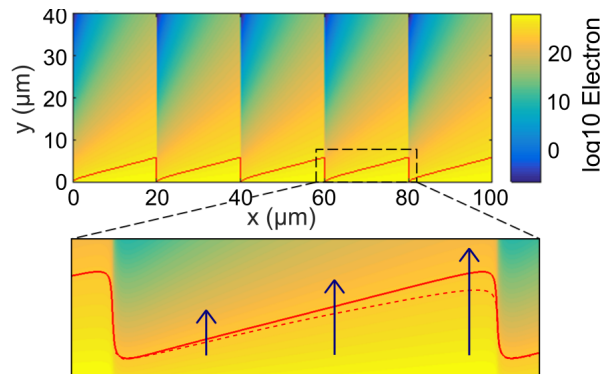


Figure 6: The plasma density structure produced from the rounded sawtooth function, and [closeup] the effect of the periodic varying of the scale length.

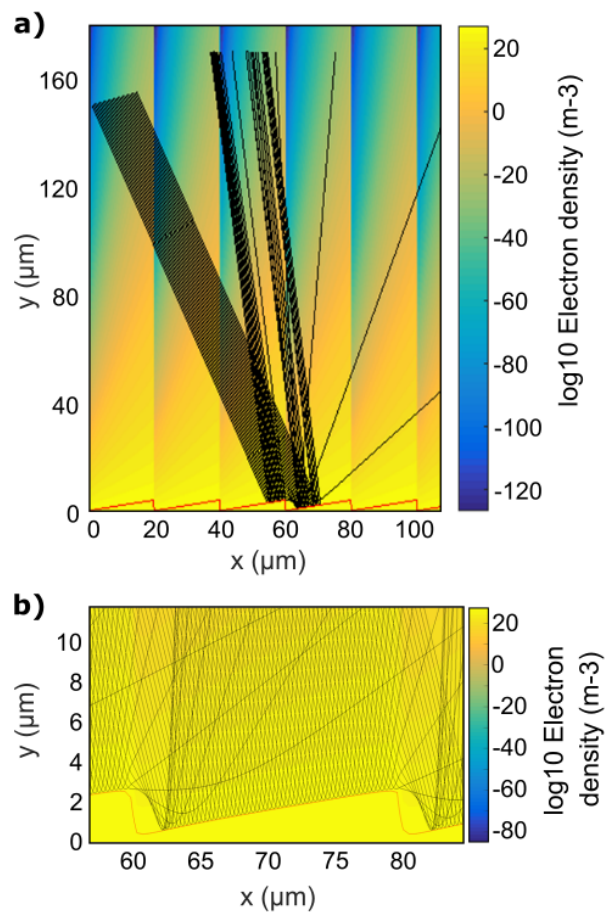


Figure 7: [a] Ray trace from a rounded sawtooth structure. It can be seen that the majority of the rays are reflected in the same direction. [b] Close up of the sawtooth ray trace, showing how the edges of the sawtooth peaks bend the paths of the rays travelling close to them.

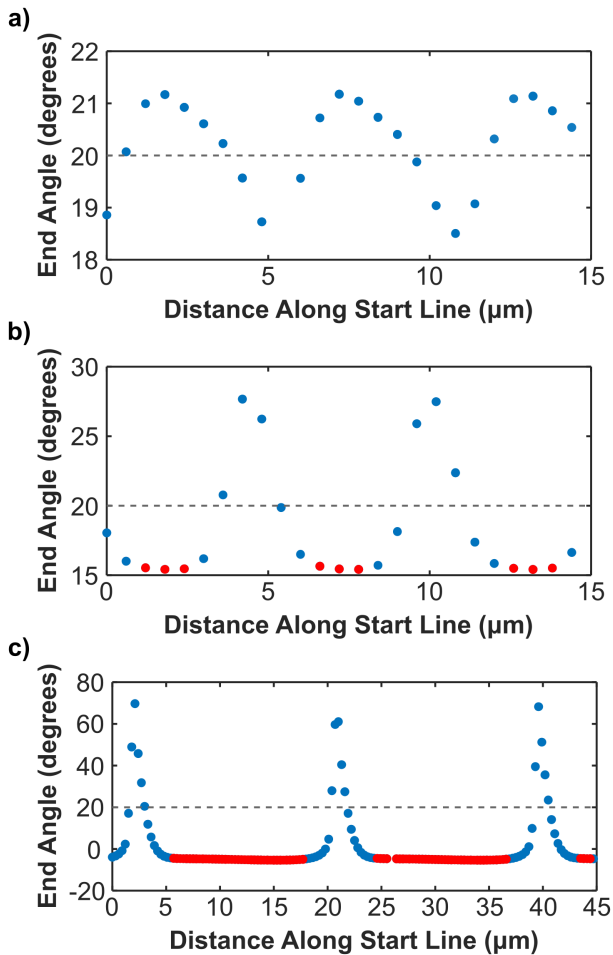


Figure 8: The angles of rays after being reflected from the grating structure, plotted against their position in the incident ray. The grating periods are [a] 1 μm , [b] 4 μm , and [c] 20 μm . All the rays are incident at 20°; this angle is shown by the dashed grey lines to indicate the angle of reflection from a mirror.

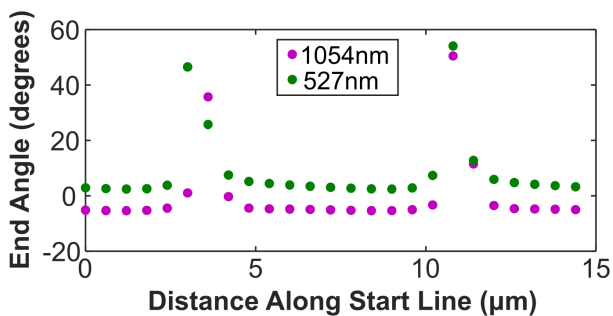


Figure 9: The angle at which rays are deflected for two different wavelengths incident on the same grating structure.

Further Work

To take this further, a more realistically expanding plasma model would be useful. At the moment, the sawtooth wave model has the plasma expanding only in the y direction, whereas it would actually expand perpendicular to the surface at each point.

Another key piece of further work is to look into whether and how it would be possible to produce the sawtooth shape in a real plasma.

Conclusion

Ray tracing in MATLAB can be used to simulate the effect of plasma mirrors and gratings on incident light rays. Investigation of a number of different potential plasma grating structures has shown that ray paths are very sensitive near the turning point to inhomogeneities in the plasma. This means that structures that could feasibly be produced by the interference of beams, such as a sinusoid and a Fourier series triangular waveform, will not act as effective, efficient plasma gratings. However, if a sawtooth structure could be produced, this could be effective as a >80% efficient plasma grating.

Acknowledgements

This work was funded through the EPSRC ASail grant number EP/K022415/1

References

- [1] C Ziener et al, J. Appl. Phys. 93, 1, 2003, *Specular reflectivity of plasma mirrors as a function of intensity, pulse duration and angle of incidence*
- [2] G Scott et al, New J. Physics, 17, 033027, 2015, *Optimization of plasma mirror reflectivity and optical quality using double laser pulses*
- [3] S Monchocé et al, Phys. Rev. Lett. 112, 145008, 2014, *Optically controlled solid-density transient plasma gratings*
- [4] L Grant-Fosrer, Annual Report 2017-18, *Optical reflection on a plasma surface*
- [5] StackExchange user *ybeltukov* <http://mathematica.stackexchange.com/questions/38293/make-a-differentiable-smooth-sawtooth-waveform>

Appendices

A Derivation of Ray Path Equation

A.1 Finding the Equation to Solve

Snell's Law: $n_0 \sin(\theta_0) = n_1 \sin(\theta_1) = n_2 \sin(\theta_2)$ etc. (for all normals parallel to one another)

Let $\mathbf{k} = n_0 \sin(\theta_0)$, where n_0 and θ_0 are the refractive index and direction at the start point of the ray.

So for any y , θ :

$$n_{ref}(y) \sin(\theta) = k \quad (7)$$

$$\tan(\theta) = \frac{dx}{dy} \quad \text{and} \quad \tan(\theta) = \frac{\sin(\theta)}{\cos(\theta)} = \frac{\sin(\theta)}{\sqrt{1 - \sin^2(\theta)}}$$

$$\text{Therefore: } \frac{dy}{dx} = \frac{\sqrt{1 - \sin^2(\theta)}}{\sin(\theta)} = \sqrt{\frac{1}{\sin^2(\theta)} - 1} = \sqrt{\left(\frac{n_{ref}(y)}{k}\right)^2 - 1}$$

So the differential equation to solve is:

$$\frac{dy}{dx} = \sqrt{\left(\frac{n_{ref}(y)}{k}\right)^2 - 1} \quad (8)$$

The refractive index is: $n_{ref}(y) = \sqrt{1 - \frac{n_e(y)q_e^2}{\epsilon_0 m \omega^2}}$ and the electron density is: $n_e(y) = n_{e0} e^{-y/L}$

The critical density is given by $n_c = \frac{\epsilon_0 m \omega^2}{q_e^2}$

So $n_{ref}(y) = \sqrt{1 - \frac{n_{e0}}{n_c} e^{-y/L}}$

Therefore: $\frac{dy}{dx} = \frac{1}{k} \sqrt{(1 - k^2) - \frac{n_{e0}}{n_c} e^{-y/L}} \rightarrow \int dx = k \sqrt{\frac{n_c}{n_{e0}}} \int \left[\frac{n_c}{n_{e0}} (1 - k^2) - e^{-y/L} \right]^{-1/2} dy$

Let $A = k \sqrt{\frac{n_c}{n_{e0}}}$ and $B = \frac{n_c}{n_{e0}} (1 - k^2)$

So we need to solve:

$$x = A \int \frac{1}{\sqrt{B - e^{-y/L}}} dy \quad (9)$$

A.2 Finding an Equation for x

$$\text{Substitution 1: } u = e^{-y/L} \quad du = -\frac{e^{-y/L}}{L} dy = -\frac{u}{L} dy \quad \rightarrow \quad x = -LA \int \frac{1}{u\sqrt{B-u}} du$$

$$\text{Substitution 2: } w = \sqrt{B-u} \quad dw = -\frac{1}{2}(B-u)^{-1/2} du = -\frac{1}{2w} du \quad \rightarrow \quad x = \frac{2LA}{B} \int \frac{1}{1-w^2/B} dw$$

$$\text{Substitution 3: } v = \frac{w}{\sqrt{B}} \quad dv = \frac{dw}{\sqrt{B}} \quad \rightarrow \quad x = \frac{2LA}{\sqrt{B}} \int \frac{1}{1-v^2} dv$$

$$\int \frac{1}{1-v^2} dv = \operatorname{arctanh}(v) \quad \rightarrow \quad x = \frac{2LA}{\sqrt{B}} \operatorname{arctanh}(v) + C$$

Substituting back in, we get:

$$x = \frac{2LA}{\sqrt{B}} \operatorname{arctanh} \left(\sqrt{1 - \frac{e^{-y/L}}{B}} \right) + C \quad (10)$$

$$\text{Rearranging gives: } e^{-y/L} = B \left[1 - \tanh^2 \left(\frac{\sqrt{B}}{2LA} (x - C) \right) \right] = B \operatorname{sech}^2 \left(\frac{\sqrt{B}}{2LA} (x - C) \right)$$

$$y = -L \ln \left[B \operatorname{sech}^2 \left(\frac{\sqrt{B}}{2LA} (x - C) \right) \right]$$

$$y = -L \ln \left[\frac{n_c}{n_{e_0}} (1 - k^2) \operatorname{sech}^2 \left(\frac{\sqrt{1 - k^2}}{2Lk} (x - C) \right) \right] \quad (11)$$

C is found using Equation 10, and using the fact that that starting coordinates of the ray, (x_0, y_0) , are known.

$$C = x_0 - \frac{2Lk}{\sqrt{1 - k^2}} \operatorname{arctanh} \left(\sqrt{1 - \frac{n_{e_0}}{n_c} \frac{e^{-y_0/L}}{(1 - k^2)}} \right) \quad (12)$$

B Equations for Grating Waveforms

B.1 Fourier Series for a Triangular Wave

$$n_e = \left[n_c + n_{amp} \frac{8}{\pi^2} \sum_{k=0}^{(order-1)} \left((2k+1)^{-2} + (-1)^k \frac{\sin \left[\frac{2\pi}{p} (2k+1)x \right]}{(2k+1)^2} \right) \right] e^{-y/L} \quad (13)$$

B.2 Rounded Sawtooth Function

The function for a rounded sawtooth wave uses functions for rounded triangle and square waves:

$$\begin{aligned} \operatorname{trg}(x) &= 1 - \frac{2}{\pi} \arccos[(1 - \delta) \sin(2\pi x)] \\ \operatorname{sqr}(x) &= \frac{2}{\pi} \arctan \left[\frac{\sin(2\pi x)}{\delta} \right] \\ \operatorname{saw}(x) &= \frac{1}{2} \left[1 + \operatorname{trg} \left(\frac{2x - 1}{4} \right) \operatorname{sqr} \left(\frac{x}{2} \right) \right] \end{aligned} \quad (14)$$

δ is a curving parameter, equal to 0.01, or some other small number.